

# Measurement of the activity of lithium in dilute solutions in molten lithium chloride between 650° C and 800° C\*

J. LIU, J.-C. POIGNET†

CREMGP/ENSEEG UA CNRS 1212, BP 75, 38402 St. Martin d'Heres, France

Received 17 July 1989; revised 8 November 1989

The lithium activity in Li–LiCl solutions has been measured by means of potentiometry in the salt-rich region of the phase diagram. The results showed that, at temperatures up to 200° C above the melting point of LiCl, the solubility of Li was several atom-percent (from 1 to 5%), as in the case of the other alkali metals dissolved in their molten halides. But the Li–LiCl system differs from the other alkali metal–alkali halide systems in that the metal activity in the saturated solutions does not exceed 0.1. This indicates the possible formation of a stable compound by the association of Li and LiCl.

## 1. Introduction

The investigations presented in this paper arose from experiments with thermal battery operations, during which it was observed that saturated solutions of Li in molten LiCl did not seem to present any significant electronic conductivity, in discrepancy with the general case of alkali metal–molten alkali halide solutions [1]. Therefore we have decided to focus on the Li–LiCl system, beginning with activity measurements of the dissolved metal, before undertaking precise electronic conductivity determinations. Thus, the present paper deals with the results for lithium activity only.

The phenomenon of dissolution of metals in molten salts bears both industrial and fundamental interests. In industry, it affects most of the molten electrolysis classical metal preparations, such as those of Na, Li, Al. Besides, high purity metals (such as Hf, Ti, Zr, Nb etc.) will be produced in the future to an increasing extent by molten salt electrolysis, and in such processes some undesirable production of alkali metals from the solvent may be promoted by the solubility of these metals in the electrolyte. In the case of lithium, the demand for the metal is expected to grow in the 1990s for the aerospace industry (Li–Al light alloys) and for electrochemical energy storage devices (lithium batteries, thermal cells, load levelling primary batteries [2, 3]).

From the fundamental point of view, the properties of metal–molten salt solutions have been investigated for over 20 years, and the first major contribution, published by Bredig [4], presented many metal–molten salt phase diagrams and a vast review of the physico-chemical properties of the corresponding solutions (particularly the electrical conductivity). Much research

has been done since that time. In the early 1980s, Warren [5, 6] published comprehensive reviews, in which thermodynamic activity and electrical conductivity measurements were major topics, with other techniques such as neutron diffraction [7], magnetic susceptibility [8], optical absorption measurements [9]. In the case of dilute metal solutions, one of the prevailing views, in agreement with the first model proposed by Pitzer [10], is that metal dissolution yields electrons which are solvated by the molten salt in the form of F centres [11–17].

Despite the vast literature in this field, systems containing lithium are still inadequately investigated and ill understood because of the extreme reactivity of the metal. The only phase diagram we found in the literature is a partial diagram published by Nakashima *et al.* [18] which deals only with the salt-rich and the metal-rich portions of the liquidus curves. The object of the present work was to measure the activity of lithium in the salt-rich monophasic region at temperatures up to 800° C.

## 2. Experimental details

The LiCl was Prolabo Rectapur, purified further by vacuum treatment at 250° C for 2 h then at 500° C for 4 h and finally by a 4–12 h pre-electrolysis (with zero volts maintained between a Li–Bi reference electrode and an iron cathode situated in the boron nitride working compartment).

The electrochemical determinations were conducted under an argon atmosphere. The experimental setup was contained inside a stainless steel glove-box where the oxygen and moisture contents were kept less than 1.5 ppm. Any nitrogen accumulation was prevented by installation of Al–Li powder inside

\* This paper was presented in part at the Molten Salt Discussion Group Summer Meeting, Leeds (July 1989).

† Maître de Conférences, Université Joseph Fourier, Grenoble, France.

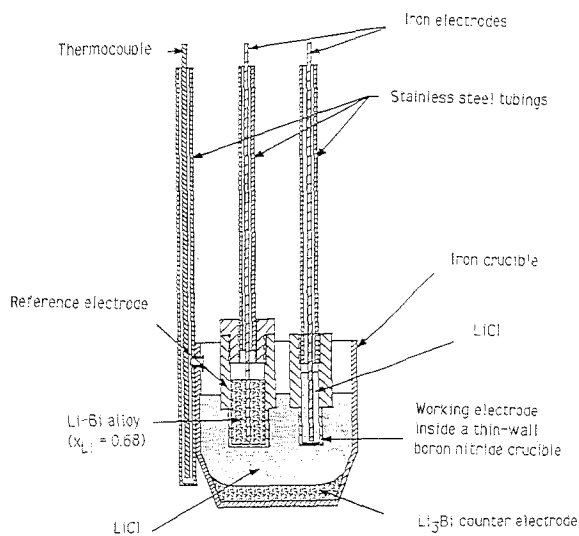


Fig. 1. Experimental arrangement of the electrodes for coulometric introduction of Li and potentiometric determination of Li activity.

the glove-box during the experiments, and evacuation of the atmosphere of the glove-box prior to each experiment.

The measurement of Li activity was performed by potentiometry. Lithium was introduced into the molten LiCl coulometrically.

The experimental arrangement is shown in Fig. 1. The reference electrode was made of a Li-Bi alloy (molar fraction of Li 0.68) contained in a thin wall boron nitride crucible which also acted as a separator. The composition of this alloy was selected, from the study of Foster *et al.* [19], to be a 2-phase region where a bismuth-rich Li-Bi solution is in equilibrium with the  $\text{Li}_3\text{Bi}$  compound. Therefore the activity of Li and the potential of the reference electrode remained constant even if the alloy composition fluctuated. This electrode proved quite satisfactory during the present work.

The working electrode was a spiral-wound iron wire placed in a known quantity of molten LiCl contained in a BN separating-crucible. A layer of  $\text{Li}_3\text{Bi}$  in the bottom part of the stainless steel crucible served as a counter-electrode.

In preparing the Li-LiCl solution, the working electrode was polarized negatively using a Par 273 potentiostat, and lithium was hence displaced from the counter-electrode to the working electrode compartment. In this compartment the electrolyte was stirred in order to facilitate the mixing of the lithium produced and the molten lithium chloride.

Once the required number of coulombs was reached, electrolysis was stopped and the potential of the working electrode with respect to the reference electrode was recorded using a Nicolet 4094C digital scope, until it reached a stable value. The whole experiment was automatically monitored by a Hewlett-Packard type 300 computer. The Li content was evaluated from the charge passed and the lithium activity was calculated from the value of the electrode potential.

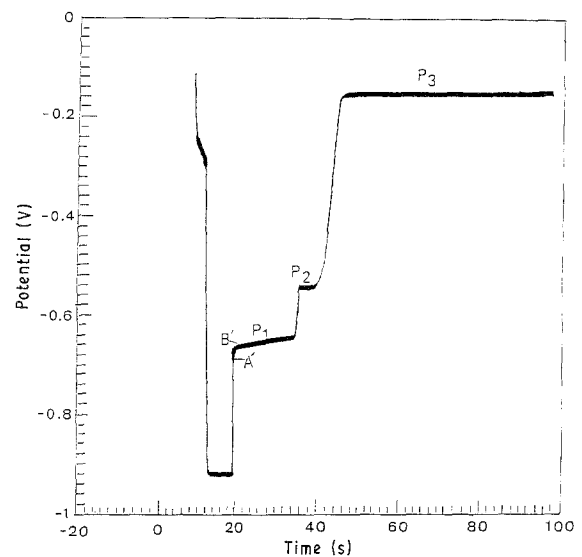


Fig. 2. Evolution of the potential of the iron electrode as lithium generated at the electrode mixes with molten LiCl, once the electrolysis has been stopped.

### 3. Results and discussion

Fig. 2 shows a typical potential-time curve during and after lithium production by electrolysis; three plateaus P1, P2 and P3 appear on the potential-time curve just after the electrolysis has been stopped. With the help of the typical phase diagrams for alkali metal-alkali halide systems [4], we may first attribute P1, P2 and P3 to pure Li, LiCl saturated with Li, and the final homogeneous solution respectively. Although this does not account perfectly for the curvature of the plot between points A' and B', such an explanation permits a first analysis of our results by direct calculation of the Li activity from the potential difference between P3 and P1.

Fig. 3 shows plots for two Li activities against their molar fractions obtained in this manner at 650°C. The first part of the curve between points A and B, which correspond to nearly zero lithium activity, was not perfectly reproducible. This may be ascribed to reac-

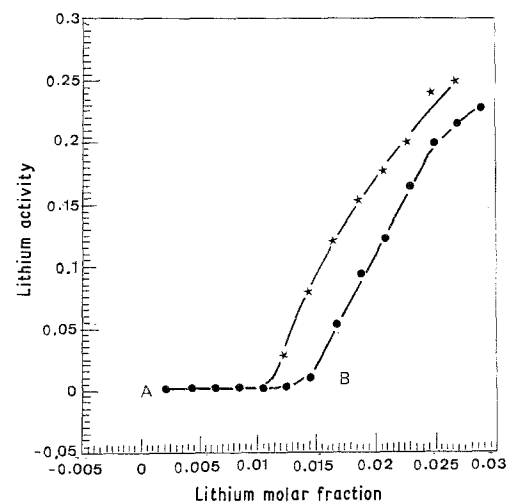


Fig. 3. Preliminary results: lithium activity against Li molar fraction in molten LiCl at 650°C.

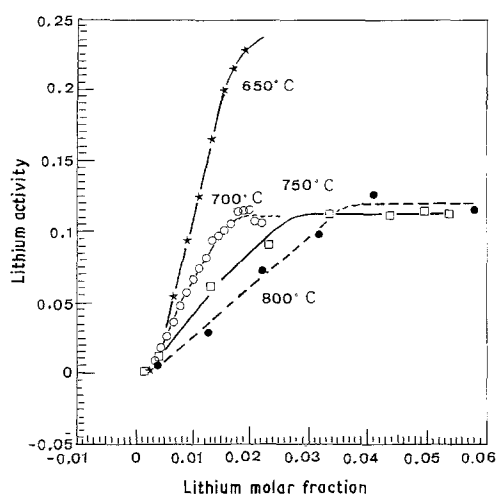


Fig. 4. Lithium activity against Li molar fraction in molten LiCl at various temperatures, after correction.

tion of the first amounts of Li produced with an impurity remaining in the working electrode compartment: we have shown, using electron microscope analysis, that traces of bismuth had migrated through the boron nitride thin wall and probably reacted with lithium in this compartment. As soon as these Bi traces had reacted, Li dissolved in the molten electrolyte. Therefore a correction for this reaction was made taking B as the zero point for the Li molar fraction. This adjustment appeared successful because the numerous curves obtained in separate experiments became reproducible once corrected. Figure 4 shows some results obtained after correction at 650°C, 700°C, 750°C and 800°C. The lithium saturation phenomenon can be clearly observed on each of these curves, which yield a Li content at saturation comparable to the results published [18]. The striking difference in saturation activities between 650°C and the higher temperatures probably corresponds to a metastable state. In fact, in the vicinity of the saturation composition, where the solution should present two phases, the nucleation energy can interfere and kinetically inhibit the formation of the second phase. In such a case, the activity measured will be higher than the equilibrium value. It may be noted that the lithium activity at saturation is about 0.1 between 700°C and 800°C, in contrast with most alkali metal-alkali halide systems, for which the corresponding values of metallic activities approach unity [5, 21].

This peculiarity of the Li-LiCl system is not consistent with a classical phase diagram with a simple miscibility gap, because in such a case the lithium activity is practically unity in the domain where two liquids are in equilibrium. The phase diagram given in [18] has been deduced from few solubility data and is very incomplete. In fact, a diagram which would include a definite compound  $\text{Li}_m\text{Cl}_n$  (Fig. 5) could offer a good explanation for the potential-time curves of Fig. 2, discussed above. In such a diagram there are two biphasic regions, situated in either side of the phase diagram; in both regions the activity of the  $\text{Li}_m\text{Cl}_n$  compound is unity, but the activity of Li,

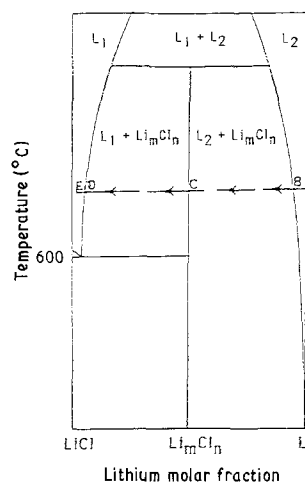


Fig. 5. Possible general shape of the Li-LiCl phase diagram, to model the experimental results.

although constant inside each region, may vary considerably when the lithium molar fraction crosses the value corresponding to the definite compound. In the present case, the lithium activity is near unity in the biphasic lithium-rich region and about 0.1 in the second region.

As already described, the explanation of the plateaus in Fig. 2 does not account for the shape of the curve between A' and B' in the same figure. Now in the case of the phase diagram of Fig. 5, this can be easily explained: after the electrolysis current has been stopped, the composition of the electrolyte in the vicinity of the working electrode changes from pure lithium to the final prepared homogeneous solution. If the solution to be prepared corresponds to point E in Fig. 5, the composition will follow the path  $A \rightarrow B \rightarrow C \rightarrow D \rightarrow E$  (Fig. 5). Between points A and B (Fig. 5), the lithium produced is surrounded by a layer of LiCl. The diffusion of LiCl and Li in opposite directions is fast because of the large composition gradient between the two layers. This rapid composition shift results in the quick, but continuous, potential increase between A' and B' in Fig. 2. The two biphasic regions between B and C and between C and D (Fig. 5) correspond to the potential plateaus P1 and P2 in Fig. 2. Finally, when the solution becomes monophasic and reaches point D (Fig. 5) we observe the last potential plateau P3 in Fig. 2.

Therefore, rather than P1, A' corresponds to the state when pure Li is on the electrode surface. The analysis of many potential-time curves showed that the potential difference between A' and the plateau P1 was  $6 \pm 2$  mV. This means that the lithium activity on plateau P1, hence on the right side of the biphasic region in Fig. 5, is between 0.90 and 0.95 at 650°C. Table 1 shows the numerical results of the lithium activity with respect to the metal molar fraction yielded by this analysis.

#### 4. Summary and conclusion

In this work, the activity of lithium in Li-LiCl solutions has been measured in a composition range

Table 1. Experimental results: lithium activities for different lithium molar fractions at various temperatures

Temperature (°C)	Li molar fraction	Li activity
650	0.002 38	0.001 20
	0.004 45	0.009 9
	0.006 49	0.052
	0.008 47	0.093
	0.010 47	0.121
	0.012 45	0.164
	0.014 42	0.198
	0.016 36	0.214
	0.018 37	0.227
	700	0.001 09
0.002 18		0.004 1
0.003 27		0.008 5
0.004 36		0.017 4
0.005 43		0.025 5
0.006 52		0.035 6
0.007 62		0.046 9
0.008 70		0.056 1
0.009 78		0.065 5
0.010 85		0.073 7
0.011 92		0.081 1
0.012 98		0.093 6
0.014 05		0.097 0
0.015 13		0.100
0.016 21		0.105
0.017 28		0.113
0.018 35	0.114	
0.019 41	0.114	
0.020 48	0.106	
0.021 54	0.105	
750	0.002 96	0.004 0
	0.012 99	0.061 1
	0.203 01	0.089 8
	0.033 01	0.112
	0.043 03	0.111
	0.053 09	0.112
800	0.002 78	0.004 0
	0.012 40	0.030 3
	0.021 90	0.072 2
	0.031 08	0.098 8
	0.040 19	0.126
	0.049 03	0.114
	0.057 77	0.115

extending from very dilute solutions to the Li-saturated solutions, at various temperatures between 650°C and 800°C. All the measurements were performed by potentiometry under pure argon atmosphere inside a stainless steel glove box. The Li–LiCl system appears

different from the other alkali metal–alkali chloride systems because the metal activity corresponding to metal-saturated solutions is not larger than 0.1 to 700°C, 750°C and 800°C, whereas it reaches unity in the case of the other alkali metal–alkali halide systems. This result could be explained if the phase diagram presented a  $\text{Li}_m\text{Cl}_n$  definite compound. The other systems only present miscibility gaps.

It will be interesting to investigate how the low activities measured can be connected to the electronic conductivity, which reaches high values in the case of the other systems [17, 20]. Results concerning the electronic conductivity of lithium–lithium chloride solutions will be presented in a subsequent paper.

## References

- [1] M. Emin, Thèse Institut National Polytechnique, Grenoble (1987).
- [2] E. Spore and B. V. Tilac, *J. Electrochem. Soc.* **134** (1987) 179.
- [3] J. W. Van Zee and E. J. Rudd, *ibid.* **135** (1988) 485.
- [4] M. A. Bredig, 'Molten Salt Chemistry' (edited by M. Blander), Interscience, New York (1964).
- [5] W. W. Warren, 'Ionic liquids, molten salts and poly-electrolytes' (edited by K. H. Benneman, F. Brouers and D. Quitman), Springer, Berlin (1982).
- [6] *Idem*, 'Advances in Molten Salt Chemistry', vol. IV (edited by G. Mamantov and J. Braunstein), Plenum Press, New York (1981) 1.
- [7] J. F. Jal, P. Chieux and J. Dupuy, *Ber. Bunsenges. Phys. Chem.* **80** (1976) 820.
- [8] R. H. Arendt and N. H. Nachtrieb, *J. Phys. Chem.* **53** (1970) 3085.
- [9] D. M. Gruen, M. Krumpelt and I. Johnson, 'Molten Salts, Characterization and Analysis' (edited by G. Mamantov), Marcel Dekker, New York (1969).
- [10] K. S. Pitzer, *J. American Soc.* **84** (1962) 2025.
- [11] N. Nicoloso and W. Freyland, *J. Phys. Chem.* **87** (1983) 1997.
- [12] W. Freyland, K. Garbade, H. Heyer and E. Pfeiffer, *ibid.* **88** (1984) 3745.
- [13] M. Parrinello and A. Rahman, *ibid.* **80** (1984) 880.
- [14] A. Selloni, R. Car, M. Parrinello and P. Carnevali, *ibid.* **91** (1987) 4947.
- [15] D. Chandler, *ibid.* **88** (1984) 3400.
- [16] M. Rovere and M. P. Tosi, *Rep. Prog. Phys.* **49** (1986) 1001.
- [17] G. M. Haarberg, K. S. Osen, J. J. Egan, H. Heyer and N. Freyland, *Ber. Bunsenges. Phys. Chem.* **92** (1988) 139.
- [18] T. Nakashima, R. Minami, K. Nakanishi and N. Watanabe, *Bull. Chem. Soc. Japan* **47** (1974) 2071.
- [19] M. S. Foster, S. E. Wood and C. E. Crouthamel, *Inorg. Chem.* **3** (1964) 1428.
- [20] J. J. Egan and W. Freyland, *Ber. Bunsenges. Phys. Chem.* **89** (1985) 381.
- [21] M. V. Smirnov, V. V. Chebikin and L. A. Tsiolkina, *Electrochim. Acta* **26** (1981) 1275.